Robust End-to-End Hand Identification via Holistic Multi-Unit Knuckle Recognition

Ritesh Vyas, Hossein Rahmani, Ricki Boswell-Challand, Plamen Angelov, Sue Black, Bryan M. Williams
Lancaster University, Lancaster, United Kingdom, LA1 4YW
r.vyas1@lancaster.ac.uk, b.williams6@lancaster.ac.uk

Abstract

In many cases of serious crime, images of a hand can be the only evidence available for the forensic identification of the offender. As well as placing them at the scene, such images and video evidence offer proof of the offender committing the crime. The knuckle creases of the human hand have emerged as an effective biometric trait and been used to identify the perpetrators of child abuse in forensic investigations. However, manual utilization of knuckle creases for identification is highly time consuming and can be subjective, requiring the expertise of experienced forensic anthropologists whose availability is very limited. Hence, there arises a need for an automated approach for localization and comparison of knuckle patterns. In this paper, we present a fully automatic end-to-end approach which localizes the minor, major and base knuckles in images of the hand, and effectively uses them for identification achieving state-of-the-art results. This work improves on existing approaches and allows us to strengthen cases further by objectively combining multiple knuckles and knuckle types to obtain a holistic matching result for comparing two hands. This yields a stronger and more robust multi-unit biometric and facilitates the large-scale examination of the potential of knuckle-based identification. Evaluated on two large landmark datasets, the proposed framework achieves equal error rates (EER) of 1.0-1.9%, rank-1 accuracies of 99.3-100% and decidability indices of 5.04-5.83. We make the full results available via a novel online GUI to raise awareness with the general public and forensic investigators about the identifiability of various knuckle regions. These strong results demonstrate the value of our holistic approach to hand identification from knuckle patterns and their utility in forensic investigations.

1. Introduction

The physiological and behavioral traits of humans can play a prominent role in identifying them [14]. The popular physiological biometric traits are the face, iris, fingerprints, and palmprints. There are also some emerging biometrics, like finger-veins and finger-knuckles, which have performed in a considerable way. The strengths of the different traits have been established to varying degrees [13]. In cases of serious crime, such as sexual abuse, video and photographic evidence is often available, which has the potential to not only place the perpetrator at the scene but record them committing the crime. More established biometrics cannot be used since the perpetrators mostly hide their faces to keep themselves anonymous, but their hands often remain visible [27]. The unique lines, creases and textures residing in the knuckle region have strong potential to provide sufficient information to distinguish the individual [15] to be used for matching evidence images to those from a suspect [26].

The finger knuckle patterns are formed on the distal interphalangeal, proximal interphalangeal and metacarpophalangeal joints of the fingers [15, 19, 22], and referred to as the major, minor and base knuckles respectively. Initial attempts at recognizing knuckle patterns were focused on the major knuckles and based on popular image processing techniques such as Gabor filters [28], Radon transforms [20, 21], phase-only correlation [29] and log-Gabor filters [4]. Moreover, existing work has largely focused on the consideration of major knuckles in the earlier years of establishing knuckles as a potential biometric. However, recent work has shown promising results from the minor and base knuckles as well [17, 19] with some recent work [5, 16] reporting good performance using deep features for the problem of knuckle recognition.

In addition to the above, automatic localization of knuckle regions from the hand-dorsal images has attracted much less attention, despite the need of this for real-world application. There is only a limited work that has reported techniques aimed at automated knuckle localization [18, 28]. These techniques work with either the images acquired from dedicated sensors [28] not typically available in forensic evidence or under controlled poses [18], which would limit their applicability for more general images. Moreover, these procedures remain highly sensitive

978-1-6654-3780-6/21/$31.00 ©2021 IEEE

to accessories (like rings) or to the accuracy of underlying steps such as edge detection. Being dependent on the finger valley points (the points at the intersection of fingers), these procedures [21, 28] become limited by variations in hand pose, which prohibits general application outside of controlled experiments. For instance, these procedures of knuckle localization fail for the hand images with touching fingers (which happens due to their inability to detect the valley points between fingers).

In addition to the above, there has been no attempt to the best of our knowledge, which evaluates the performance of knuckle recognition in a holistic manner (i.e. for all three knuckle types and all four fingers). Holistic knuckle evaluation has the potential to add high value to the overall hand recognition problem by making use of information from all of the knuckles to yield improved recognition accuracy and lower error rates.

This work presents a comprehensive end-to-end deep learning framework for robust identification from images of the dorsal side of the human hand using the knuckle creases as a biometric trait. The proposed approach processes the input hand dorsal image to detect the knuckle regions, followed by assuring anatomically-correct detection through a new quality metric. It then extracts the discerning deep features, and establishes whether there is a match, exploring the identifiability of each knuckle. Our contributions are:

1. We propose an end-to-end framework for person identification based on individual knuckles, allowing whole dorsal hand images to be considered without pre-processing. This includes improved localization that avoids common problems associated with variations in hand pose, allowing more generalisability. We extract feature vectors representing the minor, major and base knuckles and compare these to evaluate the identifiability of each knuckle on two large landmark datasets, helping us to understand the potential of each knuckle and finger.

2. We devise and incorporate an automated quality check for knuckle localization, which removes unsuitable knuckles from consideration and allows low quality images to be reported.

3. We extend this model to a holistic matching approach for identification of the whole hand using all available knuckles, resulting in more accurate and robust identification. We make the full holistic analysis of all 2^{12} knuckle combinations publicly available online (please refer to Section 3.4 for the link) in formats accessible to both scientists and the general public.

The rest of the paper is organized as follows: Section 2 presents our automated knuckle localization and end-to-end framework for biometric identification using multiple knuckles and knuckle types; Section 3 describes the experimental setup, including the employed databases, and the experimental results; Section 4 discusses the work presented and concludes the paper.

2. Proposed Framework

Here, we describe our end-to-end framework for identification from dorsal hand images using the knuckles, removing the need for human intervention. As demonstrated in Figure 1, which shows a representative block diagram for the proposed framework, our approach detects the knuckle regions, obtains the distinctive features thereof and performs the comparisons for identification. Various blocks of Fig. 1 are elucidated in the following subsections.

2.1. Knuckle localization

The majority of the knuckle detection work in the literature is derived from image characteristics and their specific poses to facilitate the detection of hand key points. In forensic identification, evidence is not limited by pose and it is not practical to manually extract each knuckle. Hence, there is a pressing need for an automated detection algorithm, robust to variations in pose, illumination and skin-tone. Data-driven approaches have demonstrated strong potential to locate regions a more generalized way. The proposed framework achieves this step through a faster region-based convolutional neural network (R-CNN) model owing to its excellent capability to yield accurate bounding boxes for the target objects in the input image [24]. The Faster R-CNN is preferred over other variants of R-CNN (baseline and Fast) due to its observed improved performance for this task and capability to obviate the computational loads posed

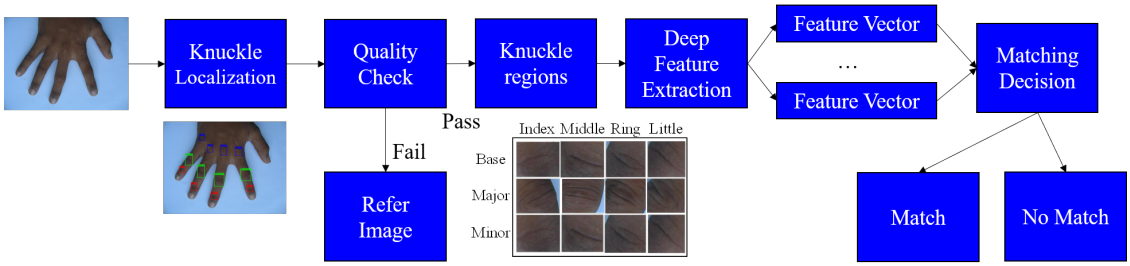

Figure 1. Overall block diagram of the proposed framework (knuckle images are rescaled for better visualization)

by selective searching used in those variants [9, 8, 10]. This is attributed to the region proposal networks (RPNs) incorporated in the Faster R-CNN, which is used for generating object detection proposals [3]. These RPNs are similar to fully convolutional networks that can predict region proposals with a wide range of scales and aspect ratios, with the help of anchor boxes as references at multiple scales and aspect ratios [24]. We thus incorporate Faster R-CNN into this framework to detect three classes (major, minor and base knuckles) and four instances of each class (one for each finger). The output of this is a collection of bounding boxes for the knuckles along with detection confidence scores and knuckle type classifications for each knuckle. Detection is achieved by selecting bounding boxes after eliminating overlapping boxes through non-maximal suppression, favoring boxes with higher thresholds. The thresholds for overlapping ratio and detection scores are chosen to be 0.5.

2.2. Quality check

Subsequent to the knuckle localization through the Faster R-CNN framework, it becomes important to assign appropriate finger labels to the detected knuckle regions. Additionally, since this paper targets the holistic evaluation of knuckle regions for overall hand identification, assigning correct finger labels proves to be of utmost importance and decisive for the overall accuracy of the system. A novel quality check is introduced here, which ensures the count and finger labels of the detected knuckle regions and correctness of their positions without having the ground truth. Under this quality metric, a check on the number of detected regions per knuckle type (major, minor and base) is applied first. There should be four detections per knuckle type pertaining to four fingers (index, middle, ring and little). As a second check, the angular directions between (major, base) and (minor, base) knuckle pairs are tested for consistency. In other words, the difference between the angular directions for these two knuckle pairs should be less than a certain threshold (determined empirically to be 10°). Subsequently, the dorsal images passing both the aforementioned quality checks are considered for the ensuing steps. This quality check prevents the poor quality hand images, such as those with no visible knuckle creases, from participating in the subsequent modules of feature extraction and matching. A small portion of the hand images fail to pass this quality check, some of which are presented in Figure 3 below. Such images are excluded from the evaluation through the approach proposed here.

2.3. Deep features

Following the quality check, the discerning features of each knuckle region are extracted and their strengths for biometric verification and identification are evaluated. For this purpose, we leverage transfer learning, whereby deep learning architectures can be trained effectively and the learnt knowledge can be mapped to a new domain in a fast and emphatic way [23, 6]. The CNN models trained on large-scale labelled data, such as ImageNet [7], can prove efficacious in learning a new task. Training such models can be much faster than the learning from scratch strategy (where the parameters of the model are initialized randomly [25]).

In this paper, transfer learning is achieved by using all but the fully connected layers of a pretrained DenseNet201 [11]. The last three layers of the model are made to accommodate the number of classes defined for the ImageNet dataset. These layers are replaced by new fully connected layers to accommodate the number of classes in the new task. Multi-class cross-entropy loss [2] is then calculated as per equation (1) and appropriate class labels are assigned for the input image.

$$loss = -\sum_{i=1}^{N}\sum_{j=1}^{K} t_{ij} \ln y_{ij} \tag{1}$$

where N and K denote the number of samples and classes, respectively. t_{ij} is an indicator that ith sample belong to jth class and y_{ij} represents the value from the softmax function, which is the probability that the ith input is associated with jth class. The pretrained model is retrained for a set of training images from the employed hand databases and used to extract the features from the test images. These test features are then compared to yield the biometrics performance metrics. A detailed discussion on the retraining of CNN model is presented in Section 3.3.

2.4. Matching

The matching of test features is accomplished through Cosine distance, where smaller values indicate more likelihood of a match and vice-versa. This matching results in genuine and imposter scores. Notably, genuine scores are the scores obtained after matching samples from the same person, whereas imposter scores are the ones obtained after matching samples from different hands. The decision threshold, which is used to distinguish accepted and rejected scores, is then varied to obtain the actual count of accepted and rejected samples, which in turn leads to calculation of metrics like false acceptance rate (FAR) and false rejection rate (FRR). Any match is said to be accepted if its matching score is below the decision threshold, otherwise it counts to the rejected matches. The definitions of performance metrics are furnished in Section 3.1.

3. Experimental setup and results

The proposed framework is tested on two large-scale public hand dorsal databases: 11k [1] and PolyU Hand-Dorsal (HD) [19]. These are the largest publicly available

hand dorsal datasets, in terms of number of images and number of subjects. These datasets are described below and the train/validation/test splits are detailed in Section 3.3.

11k dataset: This dataset consists of 11076 hand images, both in the palmar and dorsal views, from 190 subjects. The images possess varied hand poses, from far-opened fingers to semi-closed and closed fingers. All images in this dataset were captured using a USB document camera with image resolution of 1600 $\times$ 1200 pixels, keeping the hands at approximately the same distance from the camera. Since this work focuses on knuckle creases, the 2788 left and 2892 right dorsal images are used.

PolyU HD dataset: This dataset consists of 4650 hand dorsal images from the right hands of 501 subjects in a similar flat pose with open fingers. The images have a resolution of 1600 $\times$ 1200 pixels, and are captured using indoor and outdoor illuminations via a hand-held camera.

3.1. Implementation details and performance metrics

All experimentation of the proposed framework was carried out using MATLAB R2020b on a Ubuntu 18.04.3 LTS system with Nvidia GeForce RTX 2080 Ti and Intel(R) Xeon(R) W-2245 CPU @ 3.90GHz processor. The performance is evaluated using the equal error rate (EER), genuine acceptance rate (GAR), false acceptance rate (FAR), decidability index (DI), and rank-1 accuracy (R1A) [12], given in equations (2)-(5) below. gen_sc and imp_sc represent the genuine and imposter vectors respectively, the symbols μ, σ and t denote the mean, variance (of the genuine/imposter score vector) and decision threshold respectively, and t_1 is the decision threshold when both FAR and FRR are equal. All the GAR values reported in this paper are obtained at FAR of 1%. Receiver operating characteristic (ROC) curves are also employed for presenting visual performance comparisons in verification and identification modes. Further, we introduced a customized two-fold quality metric for knuckle localization.

$$FAR(t) = \frac{length(imp\_sc < t)}{length(imp\_sc)} \tag{2}$$

$$FRR(t) = \frac{length(gen\_sc > t)}{length(gen\_sc)} \tag{3}$$

$$EER = \frac{FAR(t_1) + FRR(t_1)}{2} \tag{4}$$

$$DI = \frac{|\mu_{gen\_sc}| - |\mu_{imp\_sc}|}{2\sqrt{\sigma^2_{gen\_sc} + \sigma^2_{imp\_sc}}} \tag{5}$$

3.2. Knuckle localization

The first part of experiments is focused on automated localization of knuckle regions, which is achieved through Faster R-CNN. The knuckle detection rules specified in Section 2.1 provide a collection of bounding boxes, which are further filtered to avoid any overlapping patches, by neglecting any overlapping patch with low confidence scores. The implementation is achieved through deep learning toolbox of MATLAB, where 100 random images from each group (left/right) of 11k dataset and 200 random images from HD dataset are used for training, and rest of the images of the database are used for testing. For the purpose of training, the images are manually annotated using ImageLabelor app of MATLAB, for twelve knuckle regions: the minor, major and base knuckles each for each of the 4 fingers. Faster R-CNN is trained with these manually annotated images for 10 epochs using stochastic gradient descent with momentum, with a learning rate of 0.001. Faster R-CNN is trained with the resnet50 and resnet101 backbone architectures for 11k and HD databases, respectively, selected through visual evaluation of the results on 100 testing images.

Further, the detected knuckle regions are tested for the proposed quality check. Following the quality check, 88.7% and 91.5% images for 11k left and right dorsal subsets,

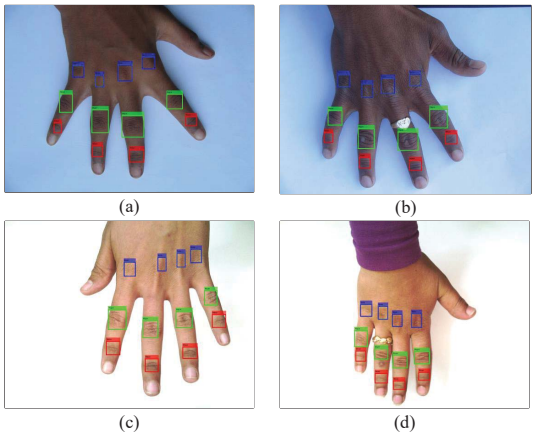

Figure 2. Sample knuckle localization for (top row) HD dataset, (bottom row) 11k dataset

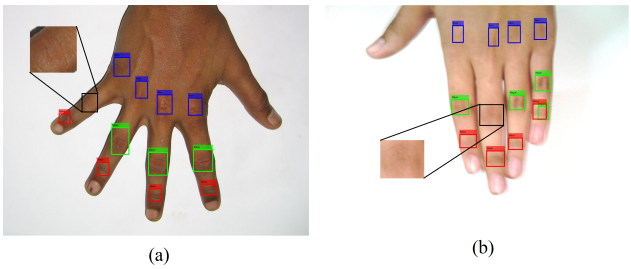

Figure 3. Samples where proposed knuckle localization fails for (a) HD dataset, (b) 11k dataset. Undetected knuckles are shown in black-edged boxes.

respectively, passed the quality checks. 95% of the HD dataset images passed the quality checks. This indicates that the identification experiments can be conducted on major portion of each dataset. Figure 2 illustrates the localization results for some of the samples from the employed datasets achieved with the proposed method, demonstrating that the proposed knuckle localization method is effective for both the challenging databases. It can be observed from the figure that the method detects the knuckle regions even in the presence of rings (Fig. 2(b,d)) and high variations in illumination (Fig. 2(c)) and skintone (Fig. 2(b)). The figure also shows that the proposed method works well for different hand poses (i.e. from pose with touching fingers (Figs. 2(d)) to pose with fingers wide open (Fig. 2(a,c))). These samples of knuckle localization clearly establishes the potential of the proposed Faster R-CNN based approach. Nevertheless, the proposed framework fails to detect the knuckle regions in small proportion of images, which happens primarily due to the poor quality of those images. Instances of such images are illustrated in Fig. 3, where the undetected knuckle regions are shown in zoomed-in versions. It can be observed from these zoomed-in versions that the undetected knuckle regions do not possess comparable features and hence are unlikely to be identifiable.

3.3. Feature extraction and biometric evaluation

The proposed framework is built upon pretrained DenseNet201 [11] for extraction of deep knuckle features, which is chosen empirically after analyzing features from other CNN models like VGG16, AlexNet, GoogLeNet and ResNet. The outperforming nature of DenseNet201 can be attributed to its deeper architecture and dense connections between the layers. Moreover, the feature reuse capability of DenseNet cause increased variations in the input of the subsequent layers, hence leading to attainment of distinctive features.

Regarding the fine tuning of pretrained DenseNet201, weights of the initial 10 layers are frozen before training. The training is carried out with stochastic gradient descent with momentum optimizer, with samples shuffled at each epoch, mini batchsize of 10 and trained for 10 epochs. The feature extraction network is fine tuned with a learning rate of 3×10^{-4} and learning rate factor of 10 for the weights and bias of the new fully connected layer. Moreover, the

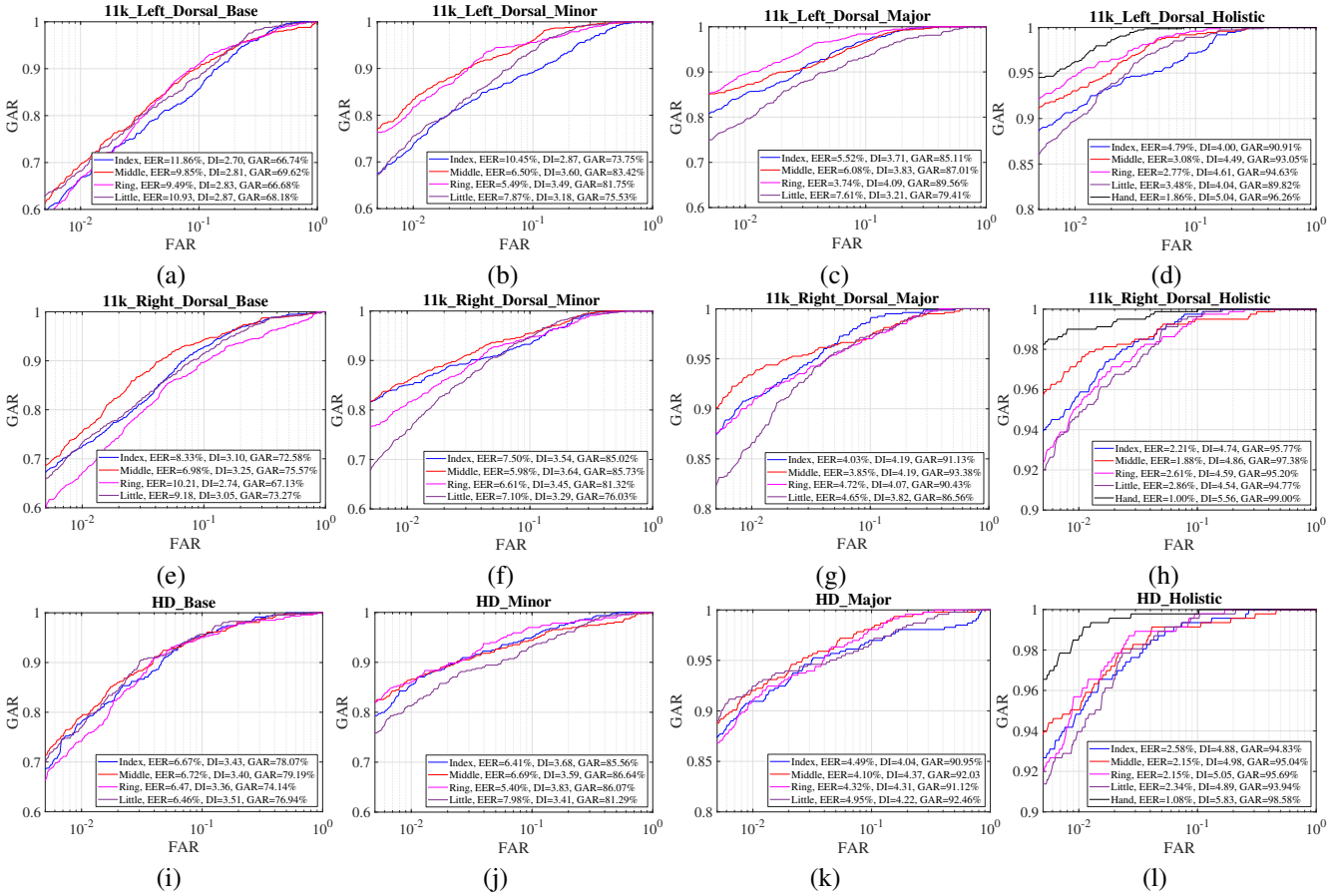

Figure 4. Receiver operating characteristics (ROC) curves for (a-d) 11k_Left dataset, (e-h) 11k_Right dataset, (i-l) HD dataset

weights of new fully connected layer are initialized using a Glorot initializer (i.e. from a uniform distribution with zero mean and variance $2/(InputSize + OutputSize)$. In order to mitigate the problem of smaller training data, several types of augmentations are applied to the training samples before the fine-tuning, including randomized reflection in the x-direction, randomized rotation in angular range of [-30° 30°], randomized translation in horizontal and vertical directions in pixel range [-30 30], and randomized scaling in both directions in scale range [0.9 1.1]. These augmentations enrich the training data with indicative variations, resulting in improved learning of the model. In addition to this, the available knuckle data is divided into training, validation and testing sets in the proportion of 60, 20 and 20 percent of the overall images. As a result, the number of images per class used for training, validation and testing are (5,2, 2), respectively for the HD dataset. Whereas, for the 11k dataset, which has varying number of samples per class, these numbers are presented as the average number of images ((9, 3, 3) for 11k_Right and (8, 3, 3) for 11k_Left datasets, respectively). Subsequently, deep features are extracted by employing the outputs of the global average pooling layer, which returns feature vectors of dimension 1×1920. The features from only the test data are employed for evaluating the performance of the proposed framework in both the verification and identification modes of biometrics. There are total 464 true and 404986 false pairs for the HD dataset, 748 true and 119547 false pairs for the 11k_Left dataset, and 801 true and 137800 false pairs for the 11k_Right dataset.

The receiver operating characteristic (ROC) curves corresponding to different knuckles of the two employed databases are depicted in Fig. 4. The values of performance metrics are also presented within these curves. Figs. 4(a,e,i) show the ROC curves for base knuckles of Left, Right dorsal subsets of 11k and for the HD dataset, respectively. It could be observed from these figures that the identifiability of base knuckles is relatively poor with high values of EER and low values of GAR. However, it is worth noting that GAR of base knuckles from the middle finger is improved over the other fingers. Notably, the GAR of base knuckles from middle finger is 69.62%, 75.57% and 79.19% for the 11k Left Dorsal, 11k Right Dorsal and HD datasets, respectively. The higher values for HD dataset can be attributed to strong creases present in the base knuckle region and the underlying acquisition setup. The ROC curves for minor knuckles are presented in Figs. 4(b,f,j), where it can be undoubtedly argued that minor knuckles are more identifiable as compared against the base knuckles. Additionally, minor knuckle from middle finger is more discerning when compared with that of other fingers. Though, it performs comparable to the index and ring fingers for 11k Right Dorsal and HD dataset, respectively, owing to possession of similar level of features.

Figures 4(c,g,k) constitute the ROC curves from major knuckles of different fingers from the 11k Left, 11k Right Dorsal and HD datasets, respectively. The EER values for major knuckles could be observed to fall as low as 3.74% for ring finger of 11k Left, 3.85% for 11k Right and 4.10% for HD dataset, proving the high identification potential of major knuckles. Furthermore, the major knuckle of little fingers from 11k dataset are the worst among all fingers. This can be justified with their least distinguishing capability as well as with their blurred acquisition in a high number of images of the dataset. However, the major knuckles from other three fingers have shown sufficient identifiability from both the multi-ethnic databases.

3.4. Holistic evaluation

An important study performed here concerns the individual identifiability of each finger in a holistic approach, which incorporates the combination of the performances of all three knuckles pertaining to a specific finger. This holistic calculation is achieved through score-level fusion via averaging. As a result, it can be observed from ROC curves of Figs. 4(d,h,l) that holistic performance of every finger from both the databases outperform the individual knuckle's performance comprehensively. This outperform-

Table 1. Rank-1 identification accuracy (%)

Finger	Knuckle	11k_Left	11k_Right	HD
Index	**Base**	78.82	84.82	62.38
	Major	93.28	93.93	91.23
	Minor	86.35	89.56	74.81
	Holistic	**98.37**	**98.29**	**95.56**
Middle	**Base**	84.32	85.96	61.49
	Major	94.70	95.26	88.90
	Minor	93.69	93.17	84.57
	Holistic	**98.98**	**98.67**	**95.12**
Ring	**Base**	76.99	73.62	57.16
	Major	94.30	92.03	90.34
	Minor	91.45	89.56	80.80
	Holistic	**97.76**	**98.10**	**95.23**
Little	**Base**	83.71	81.78	59.16
	Major	88.59	86.34	88.57
	Minor	83.91	80.83	73.25
	Holistic	**97.15**	**96.58**	**92.79**
Hand	**All**	**100**	**99.62**	**99.33**

ing nature can be observed in all the listed performance metrics. Hence, it can be deduced that having the localization of all three knuckles from a particular finger with reasonable confidence, could lead to higher distinguishing capability of that finger as a whole. This idea could prove decisive in real-life perpetrator identification cases. In addition, Figs. 4(d,h,l) present the ROC curves for the entire hand i.e. combining the scores from holistic performances of all four fingers. These ROC curves corresponding to whole hands illustrate excellent identifiability with EER as low as around 1% given good localization of the twelve knuckle regions which validates the premise of the proposed approach.

The rank-1 identification accuracy for different knuckles and fingers are reported in Table 1. These results prove the efficacy of the proposed framework in the identification mode of biometrics. In compliance with the verification experiments described above, the identification experiments also validate the fact that the major knuckle of all fingers are the most distinguishing knuckles, yielding rank-1 accuracies of the order of 93-95% for all fingers, except the little finger. In addition, the rank-1 identification accuracy for the holistic experiments exhibit encouraging results, with values as high as 97%. These high values prove that despite the contactless acquisition of dorsal views of hands in both the databases, identification can be performed with high accuracy if all three knuckles of any finger can be made available for the purpose. Whereas, the last row of Table 1 sets forth the rank-1 identification accuracy for the full-hands, which are achieved by combining the matching scores from holistic finger performances. These high values of the order of 99-100% demonstrate the promising nature of the proposed framework for both the employed databases.

A separate tabular representation of performance metrics for combination of individual knuckle types (base, major and minor) is given in Table 2. The table re-establishes the fact that major knuckles are the most identifiable knuckle type, through the consistent low values of EER for both the employed datasets (1.73% and 0.97% for 11k left and right, and 1.13% for HD database, respectively). Concurrently, better values of other metrics, like DI, GAR and R1A, support this inference. The second best identifiability is exhibited by the minor knuckles for 11k dataset with respective EERs of 2.80%, 2.86% and by base knuckles for HD dataset with EER of 2.16%. Hence, Tables 1 and 2 provide strong testimony in vindication of the proposed holistic evaluation. Additionally, we also bring the full holistic analysis in the public domain through the following link: https://h-unique.lancaster.ac.uk/performance/

The cross-domain experiments are also conducted to evaluate images from the 11k_Right subset (as HD dataset consists of images from the right hand only) on the models trained with images from the HD dataset and vice-versa. The obtained EERs for the holistic matching case in both the cross-domain evaluation scenarios (HD vs. 11k_Right and 11k_Right vs. HD) are 5.35% and 8.78%, respectively. These good EER values indicate that the proposed approach is well generalizable.

3.5. Comparison

The proposed approach is the first attempt to evaluate the knuckle recognition for 11k. For HD, results of the proposed approach are compared against those of Kumar and Xu [19]. In their paper, the EERs for base knuckles were provided as 20.87%, 18.47%, 23.17% and 22.84% for the index, middle, ring and little fingers, respectively. These values are clearly inferior as compared to the EERs achieved with the proposed approach, which are 6.67%, 6.72%, 6.47% and 6.46% for the respective fingers. Additionally, the work in [19] presented ROC curves for individual knuckle types and their combinations pertaining to each finger. The best GAR values (estimated visually from the ROC curves) of their work are found to fall in the range of 75-80%, 78-83%, 77-82% and 73-78% for the index, middle, ring and little fingers, respectively. Whereas, the best GARs for the proposed approach are 94.83%, 95.04%, 95.69% and 93.94% for the respective fingers (see Fig. 2(l)). Hence, the proposed approach outperforms state-of-the-art knuckle recognition.

4. Conclusion

This paper proposes an end-to-end deep learning framework for hand identification using all of the knuckles. The proposed method initiates with knuckle localization of the input hand image, followed by the quality check. This pro-

Table 2. Performance metrics for individual knuckle types combined over the fingers

Dataset / Knuckle	11k-Left				11k-Right				HD			
	EER(%)	**DI**	**GAR(%)**	**R1A(%)**	**EER(%)**	**DI**	**GAR(%)**	**R1A(%)**	**EER(%)**	**DI**	**GAR(%)**	**R1A(%)**
Base	5.87	3.74	86.36	96.95	4.07	4.06	89.26	95.64	2.16	4.83	94.83	89.12
Major	**1.73**	**5.04**	**96.78**	**99.80**	**0.97**	**5.67**	**99.13**	**99.43**	**1.13**	**5.68**	**98.26**	**98.34**
Minor	2.80	4.38	93.43	99.19	2.86	4.68	95.26	98.29	3.08	4.85	94.18	96.34
Hand	**1.86**	**5.04**	**96.26**	**100**	**1.00**	**5.56**	**99.00**	**99.62**	**1.08**	**5.83**	**98.58**	**99.33**

cedure is the first of its kind for knuckle localization and the inclusion of a two-fold quality metric, allowing the model to largely consider hand images with appropriate localization and refer images that are not likely to be identifiable. Thereafter, the proposed framework extracts the discerning features of various knuckles through retraining of pretrained CNN model. These extracted features are then employed to establish the identifiability of all knuckles, fingers and hand as a whole. To the best of authors' knowledge, this is the first approach for person identification using knuckle creases holistically which actually allows for whole-hand identification robustly with impressive results.

References

[1] M. Afifi. 11K Hands: Gender Recognition and Biometric Identification Using a Large Dataset of Hand Images. *Multimed Tools Appl*, 78:20835–20854, 2019.

[2] C. M. Bishop. *Pattern Recognit Mach Learning*. Springer, Singapore, 2006.

[3] Y. Chen, W. Li, C. Sakaridis, D. Dai, and L. Van Gool. Domain Adaptive Faster R-CNN for Object Detection in the Wild. In *Proc IEEE Comput Soc Conf Comput Vis Pattern Recognit*, pages 3339–3348, 2018.

[4] K. Cheng and A. Kumar. Contactless finger knuckle identification using smartphones. In *Proc Int Conf Biometrics Special Interest Group, BIOSIG 2012*, pages 1–6. IEEE, 2012.

[5] K. H. Cheng and A. Kumar. Deep Feature Collaboration for Challenging 3D Finger Knuckle Identification. *IEEE Trans Inf Forensics Secur*, 16:1158–1173, 2021.

[6] S. H. Choudhury, A. Kumar, and S. H. Laskar. Biometric Authentication through Unification of Finger Dorsal Biometric Traits. *Inf Sci*, 497:202–218, 2019.

[7] J. Deng, W. Dong, R. Socher, L.-J. Li, K. Li, and L. Fei-Fei. ImageNet: Constructing a large-scale image database. In *2009 IEEE Conf Comput Vis Pattern Recognit*, pages 248–255, 2009.

[8] R. Girshick. Fast R-CNN. In *Proceedings of the IEEE Int Conf Comput Vis*, pages 1440–1448, 2015.

[9] R. Girshick, J. Donahue, T. Darrell, and J. Malik. Rich feature hierarchies for accurate object detection and semantic segmentation. In *Proc IEEE Comput Soc Conf Comput Vis Pattern Recognit*, pages 580–587, 2014.

[10] R. Girshick, J. Donahue, T. Darrell, and J. Malik. Region-Based Convolutional Networks for Accurate Object Detection and Segmentation. *IEEE Trans Pattern Anal Mach Intell*, 38(1):142–158, 2016.

[11] G. Huang, Z. Liu, L. van der Maaten, and K. Q. Weinberger. Densely Connected Convolutional Networks. In *Proceedings of the IEEE Conf Comput Vis Pattern Recognit*, pages 4700–4708, 2017.

[12] A. K. Jain, P. Flynn, and A. A. Ross. *Handbook of Biometrics*. 2008.

[13] A. K. Jain, K. Nandakumar, and A. Ross. 50 years of biometric research: Accomplishments, challenges, and opportunities. *Pattern Recognit Lett*, 79:80–105, 2016.

[14] A. K. Jain, A. Ross, and S. Prabhakar. An Introduction to Biometric Recognition. *IEEE Trans Circuits Syst Video Technol*, 14(1):4–20, jan 2004.

[15] G. Jaswal, A. Kaul, and R. Nath. Knuckle print biometrics and fusion schemes - Overview, challenges, and solutions. *ACM Computing Surveys*, 49(2), 2016.

[16] G. Jaswal, A. Nigam, and R. Nath. DeepKnuckle: revealing the human identity. *Multimed Tools Appl*, 76(18):18955–18984, 2017.

[17] A. Kumar. Importance of being unique from finger dorsal patterns: Exploring minor finger knuckle patterns in verifying human identities. *IEEE Trans Inf Forensics Secur*, 9(8):1288–1298, 2014.

[18] A. Kumar and C. Ravikanth. Personal authentication using finger knuckle surface. *IEEE Trans Inf Forensics Secur*, 4(1):98–110, 2009.

[19] A. Kumar and Z. Xu. Personal Identification Using Minor Knuckle Patterns from Palm Dorsal Surface. *IEEE Trans Inf Forensics Secur*, 11(10):2338–2348, 2016.

[20] A. Kumar and Y. Zhou. Human identification using KnuckleCodes. In *IEEE 3rd Int Conf Biometrics: Theory, Applications and Systems, BTAS 2009*, pages 1–6, 2009.

[21] A. Kumar and Y. Zhou. Personal identification using finger knuckle orientation features. *Electronics Letters*, 45(20):1023–1025, 2009.

[22] G. K. O. Michael, T. Connie, and A. T. B. Jin. Robust palm print and knuckle print recognition system using a contactless approach. In *5th IEEE Conf Ind Electron Appl (ICIEA)*, pages 323–329, 2010.

[23] S. J. Pan and Q. Yang. A survey on transfer learning. *IEEE Trans Knowl Data Eng*, 22(10):1345–1359, 2010.

[24] S. Ren, K. He, R. Girshick, and J. Sun. Faster R-CNN: Towards Real-Time Object Detection with Region Proposal Networks. *IEEE Trans Pattern Anal Mach Intell*, 39(6):1137–1149, 2016.

[25] H. C. Shin, H. R. Roth, M. Gao, L. Lu, Z. Xu, I. Nogues, J. Yao, D. Mollura, and R. M. Summers. Deep Convolutional Neural Networks for Computer-Aided Detection: CNN Architectures, Dataset Characteristics and Transfer Learning. *IEEE Trans Med Imaging*, 35(5):1285–1298, 2016.

[26] The Guardian. Paedophile Identified by Freckles on His Hands Jailed for Six Years. https://www.theguardian.com/society/2009/apr/23/paedophile-thailand-freckles-dean-hardy.

[27] Wired. To catch a paedophile, you only need to look at their hands. https://www.wired.co.uk/article/sue-black-forensics-hand-markings-paedophiles-rapists.

[28] L. Zhang, L. Zhang, D. Zhang, and H. Zhu. Online finger-knuckle-print verification for personal authentication. *Pattern Recognit*, 43(7):2560–2571, 2010.

[29] L. Zhang, L. Zhang, D. Zhang, and H. Zhu. Ensemble of local and global information for fingerknuckle-print recognition. *Pattern Recognit*, 44(9):1990–1998, 2011.